

Analytical and Numerical Investigation of FGM Pressure Vessel Reinforced by Laminated Composite Materials

A.R Ghasemi*, A. Kazemian, M. Moradi

Department of Mechanical Engineering, University of Kashan, Kashan, Iran

Received 3 September 2013; accepted 8 December 2013

ABSTRACT

In this research, the analytical and numerical investigation of a cylindrical shell made of functionally graded materials (FGMs) reinforced by laminated composite subjected to internal pressure is presented. Using the infinitesimal theory of elasticity, the analytical solution of stress and strain in vessels made of FGMs is studied first. It is assumed that the elasticity modulus follows a power law distribution in the thickness direction and Poisson's ratio considered to be constant for simplicity. The results of the finite element method using ABAQUS software for in-homogeneity constant β in the range of -2 to 2 have been compared with the analytical results. The comparison represents good coincidence between analytical and numerical results and confirms the accuracy of stress and strain solutions presented for vessel made of FGMs. The stress and strain solutions in laminated composite vessels are then investigated. Finally, modeling of FGM vessel reinforced by composite laminates with different lay-up is taken into consideration. The obtained results demonstrate that in the cylindrical shell reinforced by laminated composites, the maximum stress is considerably less than the maximum stress in the pressure vessels made of just composites or FGMs.

© 2014 IAU, Arak Branch. All rights reserved.

Keywords: Stress analysis; Cylindrical pressure vessels; FGM; Composite; Finite element

1 INTRODUCTION

NOWADAYS with ever-increasing industrial development, pressure vessels and pipes are widely used in reactor technology, chemical industries, marine and aerospace engineering. Since in most applications, vessels must operate under extremes of thermal and mechanical loadings, any failure or fracture will be an irreparable disaster. So, adequate strength consideration is so important for these components.

Composite materials are suitable candidate for use in pressure vessel. For example, Adali et al. presented an exact solution method for optimization of laminated composite vessels under internal pressure [1]. They obtained a three-dimensional theory for anisotropic composite thick-walled cylinders subjected to symmetric loads. Optimization of pressure vessels showed that the stacking sequence can be employed for maximum burst pressure, effectively.

Mackerle presented a comprehensive review (1996-2004) of theoretical and practical analysis of pressure vessel structure/components and piping. Also, he studied different analysis, applications and components of pressure vessels [2-4]. Kabir presented internally pressurized cylindrical vessels with over-wrapped metallic liner. His analysis results showed that metallic liner causes significant decrease in on-axis stress, in both helical and circular layers [5]. Xia et al. performed the analysis of multi-layered filament-wound composite pipes subjected to internal

* Corresponding author. Tel.: +98 361 5559930; Fax: +98 361 5559930.
E-mail address: Ghasemi@kashanu.ac.ir (A.R. Ghasemi).

pressure. They presented an elastic exact solution for stress and deformation distribution of these pipes [6]. Furthermore, using 3D anisotropic elasticity, they showed that the stress and displacement distributions strongly depend on the stacking sequence.

Parnas and Nuran developed an analytical procedure to assess the behavior of a cylindrical composite structure under loading conditions particular to the rocket motor case [7]. In their study, the classical laminate theory and the generalized plane strain model were used to formulate the elasticity problem. Also, they studied different loading conditions consist of axial force and body force due to rotation, temperature and moisture variations throughout the body for a cylindrical vessel subjected to internal pressure. They analyzed a cylindrical pressure vessel using two thick-walled and thin-walled solution approaches. Then they showed that for composite pressure vessels with a radius ratio (outer to inner radius ratio) up to 1.1, two approaches give the same results in terms of the optimum winding angle and burst pressure. Also, they showed that the thick-walled analysis is required as this ratio increases [7]. Furthermore, the results showed that the maximum angular velocity is strongly influenced by the thickness of the vessel. Therefore, the thin-walled analysis is said to be an average but a safe solution.

Hocine et al. studied a vessel made of carbon/epoxy envelope coated on metallic liner, experimentally and analytically. They presented an exact solution of stresses and strains on cylindrical section of vessel under mechanical loading. Also, they validated the analytical results by manufacturing and testing some prototype vessels [8]. Stresses, strains and displacements obtained from the analytical solution [8] are in good agreement with the numerical results obtained from finite element software (ANSYS 11.0).

Baoping et al. presented the reliability-based load and resistance factor design of composite pressure vessel subjected to external hydrostatic pressure. Compared with the deterministic design methods, the probabilistic design method provides some advantages such as more accurate failure probabilities and avoids costly over-design and conservative manufacturing of composite vessels [9].

Despite many advantages of full-composite pressure vessels, they have some limitations such as stress concentration, crack at high temperature and leakage. In the other hand, functionally graded materials (FGMs) have known advantages such as smooth change of physical and mechanical properties. Recently, there has been growing interest in materials deliberately fabricated so that their mechanical properties vary continuously in space on the macroscopic scale [10]. Many studies are done by researchers on analysis of FGM pressure vessel or disc [10-13]. For example, Tutuncu and Murat presented an exact solution of stresses in FGM pressure vessels. They used infinitesimal elasticity theory and isotropic materials assumption to obtain closed-form solutions for stresses and displacements in cylindrical and spherical FGM vessels subjected to internal pressure [14]. Poisson's ratio was assumed to be constant and radially varying elastic modulus was approximated by $E(r) = E_0 r^\beta$, in which r is away from inner to outer radius. Their results showed that more stiffness is needed near the inner surface for better resistance against applied internal pressure. Thus, by decreasing the stiffness in the radial direction, stress increases compared to homogenous case.

Using the infinitesimal theory of elasticity, Dai et al. [10] obtained exact solution of FGM cylindrical and spherical vessels subjected to internal pressure and a uniform magnetic field. Same as [14] the material constants follow power functions in the radial direction. Numerical results showed that the gradient index β has a great effect on the magneto-elastic stress and perturbation of magnetic field vector.

Also, Tutuncu studied the stresses of thick-walled FGM vessels with variable exponential properties in another work and considered the exponentially-varying elastic modulus throughout thickness in the form of $E(r) = E_0 e^{\beta r}$ [15]. Shariyat et al. [11] developed analytical and numerical elasto-dynamic solutions for long thick-walled functionally graded cylinders subjected to arbitrary dynamic and shock pressures. Variations of the material properties across the thickness are described according to both polynomial and power law functions. A numerically consistent transfinite element formulation is presented for both functions whereas the exact solution is presented for the power law function. Results obtained for various exponents of the functions of the material properties distributions, various radius ratios, and various dynamic and shock loads.

Rotating disc and pressure vessel have similar steps to formulation. So using FGMs rotating disc is suitable. Ghorbanpour et al. [12-13] presented a semi-analytical solution for magneto-thermo-elasticity problem and steady state conduction heat transfer of a thin axisymmetric FG rotating disk with variable [12] and constant [13] thickness. The material properties of FG disc except Poisson's ratio modeled as the power-law distribution of volume fraction. The effects of material's grading index on the stresses, the radial displacement, the temperature, and the perturbation of magnetic field vector of the FG rotating disk had been investigated [12]. Solution for stresses and perturbation of magnetic field vector in a thin FG rotating disk is determined using infinitesimal theory of magneto-thermo-elasticity under plane stress conditions [13].

These researches show that analytical and numerical study of FGMs pressure vessel and rotating disc is done extensively but they are limited only to stress and deformation analysis. Optimization of these materials is limited to select a proper value of β in $E(r) = E_0 e^{\beta r}$. Despite of the FGMs, in composite pressure vessel using different sequential arrangement [1], coating [8] and metal liner [5] are some of optimization methods.

Survey of these articles show researchers restricted their analysis to composite pressure vessels or FGM vessels. Composite materials cause to performance improvement and material saving of vessels. However, the major disadvantage of these materials is rapid changes of interface properties of layers, which causes stress concentration, matrix cracking and delamination. Additionally carbon/epoxy composite vessels, have a lot of pores that cause leakage of component. As the FGMs are new materials with desirable properties and composite material with high strength to weight fraction, combination of these two materials is a new idea to gain FGMs advantages to improve composite disadvantages. However, a research on stress and strain distribution in hybrid vessels made of FGMs reinforced by laminated composite is a new approach to find new material with prominent properties. In this study, FGMs are used to reduce the stress concentration, control crack growth and to prevent leakage of fluid in composite pressure vessel.

For these purposes, first analytical solution of thick-walled FGM pressure vessels is considered. Then, numerical study is conducted using the ABAQUS commercial software. After that, numerical study of FGM pressure vessels reinforced by laminated composite subjected to internal pressure is accomplished. Finally, stress distribution in composite vessel, FGM vessel and hybrid vessel are compared and evaluated.

2 ANALYTICAL SOLUTION OF FGM VESSELS

FGMs vessels are thick-wall or thin-wall cylinders that contain fluids for different applications. A schematic of finite element model of the vessel is shown in Fig. 1. For a composite vessel or FGM vessel, FGM or composite thickness is zero, respectively. The radial coordinate \bar{r} and the displacement \bar{u} are normalized as $r = \bar{r}/R$ and $u = \bar{u}/R$ where R is the outer radius of the cylinder. Poisson's ratio is assumed to be constant and radially varying elastic modulus is approximated by $E(r) = E_0 r^\beta$. Since r is away from zero and ranges in (a, R) , by adjusting the constants E_0 and β , it is possible to obtain physically properties results.

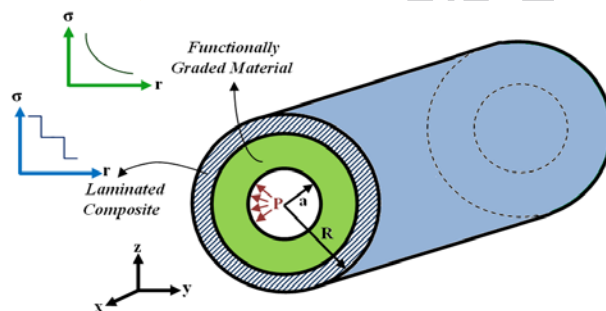


Fig. 1
Schematic of FGM pressure vessels reinforced by laminated composites subjected to internal pressure.

Assuming plane strain and axisymmetry of cylindrical coordinate problem [14-15] the only non-trivial equilibrium equation is expressed in terms of:

$$\frac{\partial \sigma_r}{\partial r} + \frac{\sigma_r - \sigma_\theta}{r} = 0 \quad (1)$$

where σ_r and σ_θ are radial and circumferential stresses, respectively. Substituting the strain-displacement relation and constitutive equation in equilibrium equations, the following equation is obtained [14-15]:

$$\frac{\partial}{\partial r} \left[\frac{E(1-\nu)r^\beta}{(1+\nu)(1-2\nu)} \left((1-\nu) \frac{\partial u_r}{\partial r} + \nu \frac{u_r}{r} \right) \right] + \frac{Er^\beta}{r(1+\nu)(1-2\nu)} \left((1-\nu) \frac{\partial u_r}{\partial r} + \nu \frac{u_r}{r} - (1-\nu) \frac{u_r}{r} - \nu \frac{\partial u_r}{\partial r} \right) = 0 \quad (2)$$

In which ν and u_r are Poisson's ratio and radial displacement, respectively. Applying differentiation and simplifying the above equation, the Cauchy-Euler equation (Eq. 3) is obtained [14-15].

$$r^2 u_r'' + (\beta+1) r u_r' + \left[\frac{\nu \beta}{(1-\nu)} - 1 \right] u_r = 0 \quad \nu^* = \frac{\nu}{(1-\nu)} \quad (3)$$

For the numerical values of $-2 \leq \beta \leq 2$ and $\nu^* = 0.3$ considered in this paper, there are only distinct real roots. For distinct real roots, the exact solution is:

$$u_r = A r^{m_1} + B r^{m_2} \quad (4)$$

And the roots of the above equation are:

$$\begin{cases} m_1 = \frac{1}{2} \left(-\beta - \sqrt{\beta^2 - 4(\nu^* \beta - 1)} \right) \\ m_2 = \frac{1}{2} \left(-\beta + \sqrt{\beta^2 - 4(\nu^* \beta - 1)} \right) \end{cases} \quad (5)$$

The constants A and B are determined from the boundary conditions. According to Fig. 1, the boundary conditions of the problem can be defined as pressure on the inner surface equal to $-P$ and zero pressure on the outer surface.

$$B.C.s \rightarrow \begin{cases} \sigma_r \left(\frac{a}{R} \right) = -P \\ \sigma_r \left(\frac{R}{R} \right) = \sigma_r(1) = 0 \end{cases} \quad (6)$$

Utilizing Eq. (6), these constants are obtained as follows [14-15]:

$$\begin{cases} A = \frac{\sigma_0}{E_0} \frac{(1+\nu)(1-2\nu)}{(1-\nu)m_1 + \nu} \\ B = -\frac{\sigma_0}{E_0} \frac{(1+\nu)(1-2\nu)}{(1-\nu)m_2 + \nu} \end{cases}, \quad \sigma_0 = -\frac{P \left(\frac{a}{R} \right)^{1-\beta}}{\left(\frac{a}{R} \right)^{m_1} - \left(\frac{a}{R} \right)^{m_2}} \quad (7)$$

Finally the expressions for the radial and circumferential stresses are derived as follows [14-15]:

$$\begin{cases} \sigma_r = \sigma_0 r^\beta (r^{m_1-1} - r^{m_2-1}) \\ \sigma_\theta = \sigma_0 r^\beta \left(\frac{(1-\nu) + \nu m_1}{(1-\nu)m_1 + \nu} r^{m_1-1} - \frac{(1-\nu) + \nu m_2}{(1-\nu)m_2 + \nu} r^{m_2-1} \right) \end{cases} \quad (8)$$

3 THICK-WALLED FGM CYLINDRICAL VESSEL MODELING

Numerical analysis of thick-walled cylindrical vessel is performed using the ABAQUS, finite element commercial software. Geometric and material properties and boundary conditions are given in Table 1. After simulation, in order to eliminate boundary conditions effects on stress values, the stress results are read far from the vessel edges. As

there isn't any defined element to model FGMs in the ABAQUS software, thick-wall cylinder partitioning method is used in form of parallel concentric cylinders. Then, according to $E(r) = E_0 r^\beta$ relation, elastic properties of each cylinder is allocated. This model is a precise approximation method to simulate the FGM vessel.

Table 1
Geometric parameters, elastic constants and boundary condition of the model

ν	E_0 (GPa)	R (mm)	a (mm)	P (MPa)
0.3	72	30	50	7

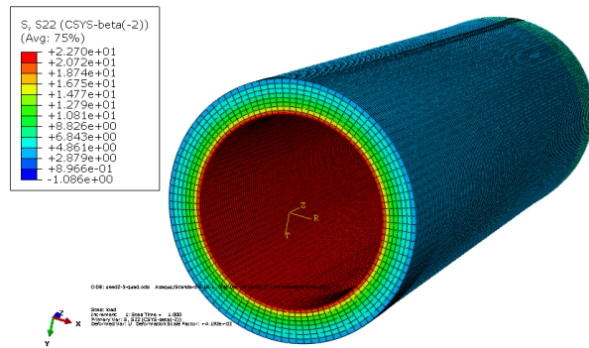


Fig. 2
Stress distribution of FGM vessel modeling under internal pressure.

Table 2
Radial and circumferential stresses of FGM cylinder for $\beta = 1$

R (mm)	Analytical[14-15]		FEM		Error (%)	
	σ_r (MPa)	σ_θ (MPa)	σ_r (MPa)	σ_θ (MPa)	σ_r (MPa)	σ_θ (MPa)
30.0	-7.00	11.17	-6.98	11.73	0.24	5.01
32.5	-5.61	10.88	-5.60	11.37	0.21	4.48
35.0	-4.44	10.67	-4.44	11.10	0.19	4.03
37.5	-3.44	10.51	-3.44	10.90	0.17	3.66
40.0	-2.57	10.40	-2.57	10.75	0.14	3.34
42.5	-1.81	10.33	-1.81	10.64	0.12	3.06
45.0	-1.14	10.28	-1.14	10.57	0.21	2.83
47.5	-0.54	10.25	-0.54	10.52	0.00	2.62
50.0	0.00	10.24	0.00	9.98	0.00	2.57

In Table 1. ν , E , a , R and P are Poisson's ratio, elastic modulus, inner radius, outer radius and internal pressure of the vessel, respectively. Modeling and simulation is done for numerical values of $\beta = -2, -1.5, 1, 2$. Stress distribution of finite element modeling of the FGM vessel is shown in Fig. 2.

Radial and circumferential stress values from the analytical solution and the finite element method (FEM), and the difference between them for in-homogeneity constant $\beta = 1$ is given in Table 2. In this table, the maximum difference between the analytical and the numerical values of the radial and the circumferential stress is about 0.24% and 5%, respectively. This difference has maximum value at the inner radius and minimum value at the outer radius. As the inner radius is subjected to pressure, Saint-Venant's principle has effected on FEM results and maximum error exists in this radius. Increase the radius made this effect decrease and the results are precise. The ratio of radial stress in the FGM shell (F) to the homogeneous shell (H) is shown in the Fig. 3. These values are obtained from the analytical solution [14-15]. The Fig. 4 shows the same stress ratio for the numerical solution using the ABAQUS finite element software. The analytical and numerical results have been depicted in two distinct figures for better illustration of differences. Also, the figures are plotted based on dimensionless r/R parameters. The similarities and results consistent between the two figures are recognizable, clearly. Thus numerical results of FEM and precise mathematical analysis have good agreement and errors always are less than 5%.

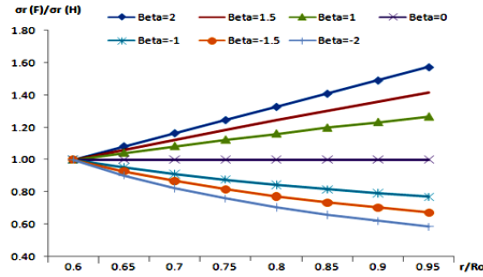


Fig. 3
Radial stress distribution in FGM cylinder using analytical method [14-15].

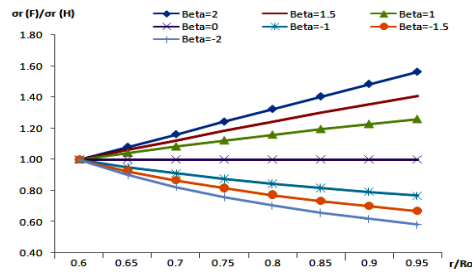


Fig. 4
Radial stress distribution in FGM cylinder using FEM.

4 MODELING FGM CYLINDRICAL SHELL REINFORCED BY COMPOSITES LAMINATES

In this section, the hybrid cylindrical model, that is FGM cylindrical shell reinforced by composite laminates, is studied. In this model, outer and inner radius of the vessel is considered to be 55 mm and 50 mm, respectively. Also, internal surface is subjected to 10 MPa pressure. The hybrid shell consists of FGM and composite laminates with thickness of 3 and 2 mm, respectively. Each FGM layer has 1 mm thickness and the its elastic properties are defined using power law relation $E(r) = E_0 r^\beta$. Furthermore, the composite part of the shell consists of four layers with 0.5 mm thickness, made of carbon/epoxy (T300/934). The elastic properties of unidirectional carbon/epoxy composite laminates are mentioned in Table 3.

Table 3
Elastic properties of unidirectional carbon/epoxy ply [16]

E_{xx} (GPa)	E_{yy} (GPa)	G_{xy} (GPa)	V_{xy}
141.6	10.3	3.88	0.268

where E_{xx} is the longitudinal modulus, E_{yy} is transverse modulus, G_{xy} is the shear modulus, and V_{xy} is the major Poisson's ratio. In order to verify the results obtained from the hybrid vessel and have a suitable comparison, FGM and full-composite vessels are modeled with 5 mm thickness. Fig. 5 shows the maximum on-axis stress distribution in FGM cylindrical shell which consists of 5 layers with 1mm thickness and in-homogeneity constant of $\beta = 2$. Also, the maximum on-axis stress distribution in a composite cylindrical shell with symmetric stacking sequences [+53/-53]_{10s} is shown in Fig. 6.

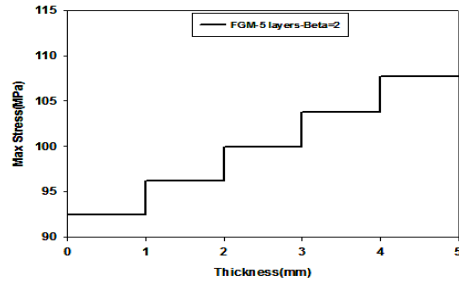


Fig. 5
Maximum principal stress distribution in FGM cylinder ($\beta = 2$).

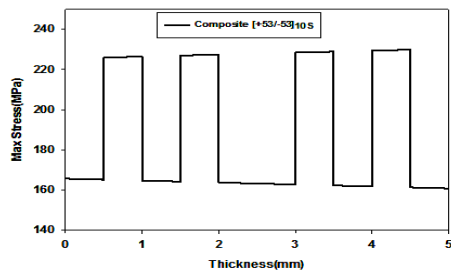


Fig. 6
Maximum on-axis stress distribution in symmetric [+53/-53]_{10S} laminated composite cylinder.

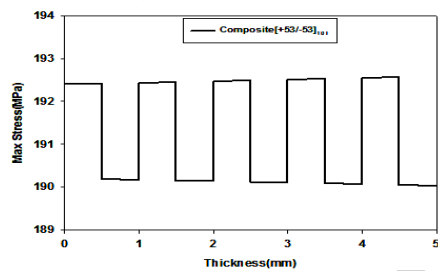


Fig. 7
Maximum on-axis stress distribution in unsymmetric [+53/-53]_{10T} laminated composite cylinder.

The stress of FGMs vessel increases from inner layer to outer layer in step form, regularly as shown in Fig.5. This step form stress started from 92.5 MPa and increased to 107.7 MPa. Also, difference between each step is almost similar (3.7 MPa). The minimum and maximum stresses in composite vessel are 163 and 228 MPa, respectively (Fig. 6). The stress distribution same as stacking sequence is symmetric.

The distribution of on-axis stress for unsymmetric layup [+53 /-53]_{10T} is shown in Fig.7. The minimum and maximum on-axis stresses in fiber direction for this layup are almost 190 MPa and 192.4 MPa, respectively. Clearly, the stress fluctuation in this arrangement is much less than symmetric layup. Furthermore, comparisons of these three figures show that the stresses in the composite shell are higher than FGM shells. In the composite cylinder all the laminates have the same orthotropic properties, whereas in FGM cylinder, material properties aren't constant and improve throughout the thickness. This material changes are the main reason of decrease and control stress in the FGM vessels.

The stress distribution in the hybrid FGM-Laminated composite vessel is different. Figs. 8 and 9 show the maximum stress distribution in hybrid cylindrical FGM shells reinforced by symmetrical and unsymmetrical laminated composite materials, respectively. In these models in-homogeneity constant is $\beta = 2$.

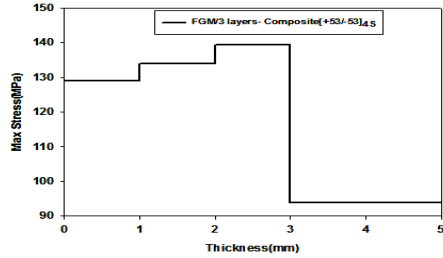


Fig. 8
Maximum stress distribution in FGM-Composite cylinder with symmetric $[+53/-53]_{4s}$ laminates ($\beta = 2$).

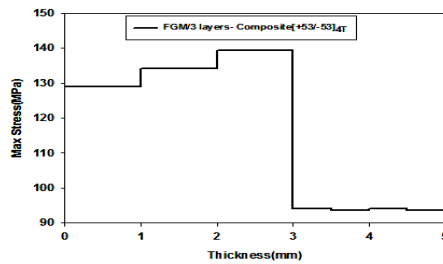


Fig. 9
Maximum stress distribution in FGM-Composite cylinder with unsymmetric $[+53/-53]_{4T}$ laminates ($\beta = 2$).

The stress distributions in the FGM part of both arrangements are the same. The stepped stresses are about 128 MPa, 135 MPa and 140 MPa. After FGM layout, there is a considerable fall in stress value in both layups. The stress of the symmetric arrangement after this fall is almost constant (93.75 MPa), whereas, the stress of the unsymmetric composite laminates oscillates between 93.5 and 94 MPa. This stress reduction and oscillation damping in the reinforced shell are significant. This is one of the benefits of the laminated composite reinforcement idea.

5 STACKING SEQUENCES EFFECTS

In this section, different stacking sequences implied to the FGM vessel to study optimization effects of these changes. First, for better comparison with the hybrid vessel, numerical analysis for laminated composite vessel with $[+55/-30]_{10s}$ and $[+55/-30]_{10T}$ layups are studied. These symmetric and unsymmetric sequences are chosen to find optimum layups. The results of this analysis are presented in Figs. 10-11.

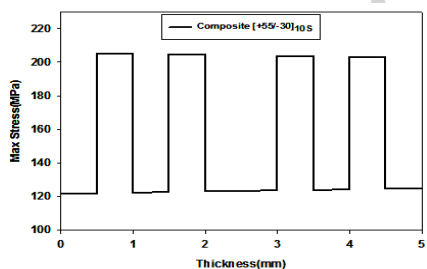


Fig. 10
Maximum on-axis stress distribution in composite cylinder with symmetric $[+55/-30]_{10s}$ layup.

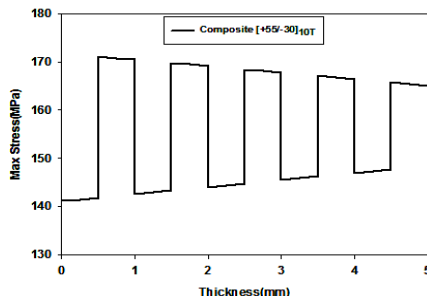


Fig. 11
Maximum on-axis stress distribution in composite cylinder with unsymmetric $[+55/-30]_{10T}$ layup.

The Fig.10 shows the maximum on-axis stresses distribution in symmetric composite cylinder with $[+55/-30]_{10S}$ layups. As it is clear from this figure, the minimum and the maximum stresses are related between 122 MPa and 129 MPa and between 203 MPa and 206 MPa, respectively. The stress distribution of unsymmetric $[+55/-30]_{10T}$ layup shows that the stresses are related almost between 140 to 170 MPa. The stress oscillation of this layup decreases along the inner plies to the outer plies. So, unsymmetric sequence has less average maximum on-axis stress and less stress change than symmetric sequence.

After the composite vessel study, hybrid FGM-laminated composite vessel using these sequences is analyzed. The stress distributions of the FGM vessel reinforced by $[+55/-30]_{4S}$ and $[+55/-30]_{4T}$ composite layups are obtained using FEM analysis and shown in Figs. 12-13.

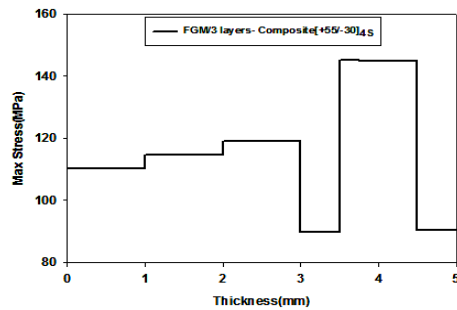


Fig. 12
Maximum stress distribution in FGM-composite cylindrical shell with symmetric $[+55/-30]_{4S}$ layup ($\beta = 2$).

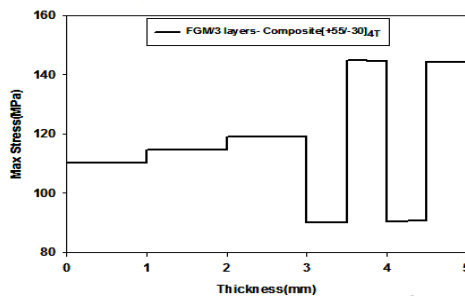


Fig. 13
Maximum stress distribution in FGM-composite cylindrical shell with unsymmetric $[+55/-30]_{4T}$ layup ($\beta = 2$).

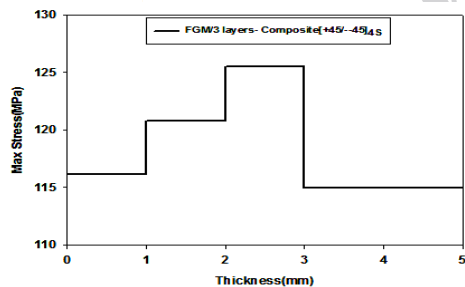


Fig.14
Maximum stress distribution in FGM-composite cylinder with symmetric $[+45/-45]_{4S}$ layup.

As shown in Figs. 12-13, the stress distribution of the FGM layers in both arrangements are equal. The stress steps of the FGMs layers are 110 MPa, 115 MPa and 119 MPa. Like the hybrid vessels studied in section 4, there is a stress fall after the FGM layers. Here, the stress is fallen to 90 MPa on the +55 degree layer; but on the -30 degree layer a significant increase up to 145 MPa can be seen.

The reason of the stress distribution differences is the symmetric and unsymmetric layups of the two stacking sequences. In the symmetric and unsymmetric layups, the stress distribution is symmetric and unsymmetric, respectively. It should be noted that the maximum stress of the FGM-composite pressure vessel is equal to the minimum stress of the composite pressure vessel. So, the FGM-composite vessel is more efficient than the composite vessel.

Furthermore, for better study of layups, another stacking sequence is considered. As the above sequences used 30° and 55° ply, 45° ply could be another choice for laminates. So, the angle-ply [+45/-45] laminated composite material is chosen for reinforcement. The stress distribution in the FGM-composite cylindrical shell with symmetric layup [+45/-45]_{4s} is shown in Fig.14.

The stresses of the FGM layers from inner to outer radius of vessel are 116 MPa, 121 MPa and 125 MPa, respectively. These stresses are a little higher than [+55/-30]_{4s} and [+55/-30]_{4T} composite layups (about 5.5%). After the FGM layers, the stress decreases throughout the composite layers up to 115 MPa. This stress drop is very significant and remains nearly constant in the laminated composite materials.

6 CONCLUSIONS

In this study, a new method to reinforce the FGM cylindrical pressure vessel by the composite laminates is presented. Analysis of the stress and the strain in the pressure vessel made of functionally graded material are studied, analytically and numerically. The results of the FEM are in good agreement with the exact solution. This results show that the FEM is sufficiently accurate for modeling the FGM vessel. In the FGM vessel the radial stress increases and the circumferential stress decreases with increasing of in-homogeneity constant between -2 and 2. Also, results show that in the hybrid vessel stress distribution depend on stacking sequences of composite cylindrical vessel, directly, so that if the layup stacking sequence is being symmetric/unsymmetric, the stress distribution is symmetric/unsymmetric, respectively. Also, the stress values of composite layers usually are very high.

In the hybrid cylindrical vessel, the stresses at the interface between the FGM and the composite layers decrease for all studied arrangements, significantly. The amount of reduction depends on layups, quietly. Among the study of different stacking sequences, [+53/-53] angles have the maximum stress reduction equal to 33% in some examples. According to the different sample modeling, it seems when the angle of reinforcing laminates approaches to the optimum angle in twisting fiber in filament winding method (almost 54.7°), the stress reduction will be further and reinforcement will done better.

ACKNOWLEDGEMENT

The authors are grateful to the University of Kashan for supporting this work by Grant No. 255980/06.

REFERENCES

- [1] Adali S., Verijenko V.E., Tabakov P.Y., Walker M., 1995, Optimization of multilayered composite pressure vessels using exact elasticity solution, ASME-Publications-PVP **302**:203-212.
- [2] Mackerle J., 1999, Finite elements in the analysis of pressure vessels and piping, an addendum, *International Journal of Pressure Vessels and Piping* **76**(7):461-485.
- [3] Mackerle J., 2002, Finite elements in the analysis of pressure vessels and piping, an addendum: a bibliography, *International Journal of Pressure Vessels and Piping* **79**(1):1-26.
- [4] Mackerle J., 2005, Finite elements in the analysis of pressure vessels and piping, an addendum: A bibliography, *International Journal of Pressure Vessels and Piping* **82**(7):571-592.
- [5] Kabir M.Z., 2000, Finite element analysis of composite pressure vessels with a load sharing metallic liner, *Composite Structures* **49**(3):247-255.
- [6] Xia M., Takayanagi H., Kemmochi K., 2001, Analysis of multi-layered filament-wound composite pipes under internal pressure, *Composite Structures* **53**(4):483-491.
- [7] Parnas L., Nuran K., 2002, Design of fiber-reinforced composite pressure vessels under various loading conditions, *Composite structures* **58**(1):83-95.
- [8] Hocine A., Chapelle D., Boubakar M. L., Benamar A., Bezazi A., 2009, Experimental and analytical investigation of the cylindrical part of a metallic vessel reinforced by filament winding while submitted to internal pressure, *International Journal of Pressure Vessels and Piping* **86**(10):649-655.
- [9] Baoping C., Liu Y., Liu Z., Tian X., Ji R., Li H., 2011, Reliability-based load and resistance factor design of composite pressure vessel under external hydrostatic pressure, *Composite Structures* **93**(11):2844-2852.
- [10] Dai H.L., Fu Y.M., Dong Z.M., 2006, Exact solution for functionally graded pressure vessels in a uniform magnetic field, *International Journal of Solids and Structures* **43**:5570-5580.
- [11] Shariyat M., Nikkhah M., Kazemi R., 2011, Exact and numerical elastodynamic solutions for thick-walled functionally graded cylinders subjected to pressure shocks, *International Journal of Pressure Vessels and Piping* **88**(2): 75-87.

- [12] Ghorbanpour Arani A., Loghman A., Shajari A.R., Amir S., 2010, Semi-analytical solution of magneto-thermo-elastic stresses for functionally graded variable thickness rotating disks, *Journal of Mechanical Science and Technology* **24**: 2107-2118.
- [13] Ghorbanpour Arani A., Amir S., 2011, Magneto-thermo-elastic stresses and perturbation of magnetic field vector in a thin functionally graded rotating disk, *Journal of Solid Mechanics* **3**(4): 392-407.
- [14] Tutuncu N., Murat O., 2001, Exact solutions for stresses in functionally graded pressure vessels, *Composites Part B: Engineering* **32**(8): 683-686.
- [15] Tutuncu N., 2007, Stresses in thick-walled FGM cylinders with exponentially-varying properties, *Engineering Structures* **29**(9):2032-2035.
- [16] Tsai S.W., 1988, *Composites Design*, 4th edition, Think Composites.

Archive of SID